ANALYSIS OF SHEAR LAYERS BASED ON THE LATTICE GAS MODEL

ATSUSHI YUASA

Advanced Technology Research Center, Mitsubishi Heavy Industries Ltd., 8–1, Sachiura 1-chome, Kanazawa-ku, Yokohama 236, Japan

TAKAJI INAMURO

Department of Chemical Engineering, Faculty of Engineering, Kyoto University, Yoshidahonmachi, Sakyo-ku, Kyoto 606-01, Japan

AND

TAKESHI ADACHI

Advanced Technology Research Center, Mitsubishi Heavy Industries Ltd., 8–1, Sachiura 1-chome, Kanazawa-ku, Yokohama 236, Japan

SUMMARY

The 'two-colour lattice gas model' is applied to the analysis of shear layers between two parallel flows with different velocities U_1 and U_2. Two cases, (a) $U_1 = 0.4$, $U_2 = 0.2$ and (b) $U_1 = 0.4$, $U_2 = 0.0$, are calculated and compared with the theoretical solutions. We obtain good agreement between theory and calculations in the velocity profiles of the shear layers. It is found that this model can simulate complicated physical phenomena of shear layers at the microscopic level.

KEY WORDS: lattice gas model; cellular automaton; shear layer; diffusion; Kelvin–Helmholtz instability

1. INTRODUCTION

In the field of computational fluid dynamics (CFD) the Navier-Stokes (N–S) equation is conventionally discretized based on the finite difference method (FDM), finite element method (FEM), etc. and is solved numerically to obtain its solution. Various numerical methods have been established in CFD in recent years and have attained great success in many fields with the simultaneous improvement in computer performance. As is well-known, the N–S equation is the governing equation of a fluid based on continuum theory in which the fluid is regarded as a macroscopic physical model. As an opposite approach, it has been suggested that a microscopic physical model called the 'cellular automaton (CA)' can be used to simulate complicated physical phenomena.[1-4] The CA comprises regular lattice arrays with discrete state variables. A system composed of CAs evolves uniformly according to predefined simple local rules. Several patterns similar to real phenomena in nature can be formed by applying these operations repeatedly.

Recently the 'lattice gas model' based on the CA has received much attention as a new computational method[5-8] because its completely discrete nature matches massively parallel hardware architecture very well.[9,10] This model imitates the motion of particles in a very simplified microscopic world in which both space and time are completely discretized. It has begun to be applied to numerical

simulations for various complicated physical phenomena[11-13] such as molecular diffusion, chemical reaction and so on.

In this paper we have used a two-colour lattice gas model[12,13] and evaluated the validity of this model by applying it to the analysis of shear layers.

2. TWO-COLOUR LATTICE GAS MODEL

We have adopted the two-dimensional 'two-colour lattice gas model'[12,13] based on the FHP model[5-7] introduced by Frisch *et al.*[5]

In the original FHP model the physical space is discretized into many regular triangular meshes and time is discretized into unit time steps. Particles with both unit mass and unit speed are located on lattice sites at integer time steps. Since the lattice is hexagonal, each particle has a velocity corresponding to one of six possible directions and moves in its velocity direction along lattice links from a certain lattice site to its nearest neighbour during a unit time step (translation process). The velocity vector c_i in the ith direction is defined as

$$c_i = \left(\cos\left(\frac{\pi i}{3}\right), \ \sin\left(\frac{\pi i}{3}\right)\right) \quad (i = 1, \ldots, 6). \tag{1}$$

In addition, we can include a 'rest particle' with zero velocity $c_0 = (0, 0)$ which stands still on lattice sites and participates in collisions. If several particles meet together on the same lattice site, a collision which conserves both the mass (the total number) and total momentum of the particles occurs and the particles instantaneously change their direction of motion (collision process). The configuration of the particles is updated at every time step by these two successive processes, as illustrated in Figure 1. Moreover, the exclusion principle is imposed, so that only one particle moving in a given direction can exist at a given site and time. Therefore the state of the particles at each site can be completely
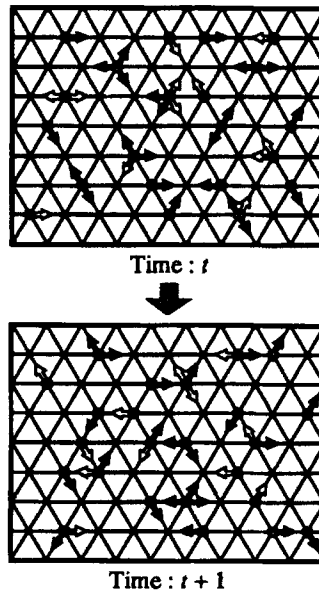

Time : t

Time : $t + 1$

Figure 1. Time evolution of particles during a unit time step in two-colour lattice gas model. Each black (white) arrow shows a red (blue) particle moving in its direction along lattice links

represented by seven Boolean variables n_i $(i = 0, \ldots, 6)$, each of which takes the value '0' or '1' according to the absence or presence of a particle with velocity c_i, respectively.

Since all particles are identical in the original model, it cannot deal with phenomena such as a mixture of different kinds of fluids. In the two-colour lattice gas model, however, two colour labels which make it possible to distinguish different particle types, e.g. 'red' and 'blue', are added to the particle states. Note that although red and blue particles can coexist at the same site, they cannot occupy the same direction at the same time in order to satisfy the exclusion principle described above.

We extended the 76 collision rules of the original FHP-III model to include two different colour labels.[12,13] There are 2084 collision rules among 3^7 possible pre-collision states and they all conserve the mass, momentum and colour of the particles at each site, as illustrated in Figures 2(a) and 2(b). Note that collision rules such as shown in Figure 2(c), which exchange only colours but do not change the colour-blind particle configuration, are also involved. If there are more than two post-collision states, one of them is selected with equal transition probability.

The Boolean variables for red and blue particles at a site at position $\mathbf{r}$ and time t are denoted by $r_i(\mathbf{r}, t)$ and $b_i(\mathbf{r}, t)$ respectively and their corresponding ensemble averages are expressed as $R_i(\mathbf{r}, t)$ and $B_i(\mathbf{r}, t)$. Thus the mean population $N_i(\mathbf{r}, t)$, which represents the average number of particles moving in the ith direction, is given as

$$N_i(\mathbf{r}, t) = R_i(\mathbf{r}, t) + B_i(\mathbf{r}, t). \tag{2}$$

As macroscopic quantities, the density ρ, mean velocity $\mathbf{u}$ and concentration of red particles, C, are defined as

$$\rho = \sum_i N_i, \tag{3}$$

$$\rho\mathbf{u} = \sum_i \mathbf{c}_i, \tag{4}$$
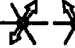
$$\rho C = \sum_i R_i. \tag{5}$$
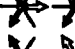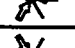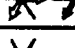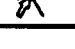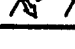
pre-collision state	post-collision state	transition probability
(a)		$\frac{1}{2}$
		$\frac{1}{2}$
		$\frac{1}{4}$
(b)		1
		1
		$\frac{1}{3}$
		$\frac{1}{3}$
(c)		1
		$\frac{1}{2}$

Figure 2. Examples of collision rules: (a) binary head-on collisions; (b) symmetrical triple collisions; (c) colour exchange collisions

The conservation laws at the microscopic level for the mass, momentum and concentration of red particles are reduced to the continuity equation, the Navier–Stokes equation and the concentration equation respectively, given as

$$\partial_t \rho + \partial_\alpha \rho u_\alpha = 0, \tag{6}$$

$$\partial_t \rho u_\alpha + \partial_\beta[\rho g(\rho) u_\alpha u_\beta] = -\partial_\alpha\left\{\tfrac{3}{7}\rho[1 - g(\rho)u^2]\right\} + \partial_\beta[v(\rho)\partial_\beta \rho u_\alpha], \tag{7}$$

$$\partial_t \rho C + \partial_\alpha \rho C u_\alpha = \partial_\alpha D(\rho)\partial_\alpha \rho C, \tag{8}$$

where $v(\rho)$ is the kinematic viscosity, $D(\rho)$ is the diffusion coefficient and $g(\rho)$ is a factor which results from the discreteness of the lattices. $v(\rho)$ and $g(\rho)$ are given as

$$v(\rho) = \frac{1}{28d(1 - d)[1 - 8d(1 - d)/7]} - \frac{1}{8}, \tag{9}$$

$$g(\rho) = \frac{7(7 - 2\rho)}{12(7 - \rho)}, \tag{10}$$

where $d = \rho/7$ is the average density per direction.

3. SIMULATION RESULTS AND DISCUSSION

3.1. Outline of numerical simulations

We applied the two-colour lattice gas model to the analysis of shear layers between two parallel flows with different velocities.

The rectangular box shown in Figure 3 is the computational domain. We divided this domain into 1024×512 triangular lattices and partitioned it into upper and lower regions of the same size, as illustrated in Figure 3. The mean velocities in the upper and lower regions are denoted by U_1 and U_2, respectively. The characteristic length is $H/2$, which is the half-width of the duct in the direction perpendicular to the flow, and the characteristic velocity is U_1, which is the faster speed in the upper region. The Reynolds number is 301 with the use of an efficient kinematic viscosity $v_{\text{eff}} = v(\rho)/g(\rho)$.

Initially the upper and lower regions are randomly filled with blue and red particles of density $\rho = 2 \cdot 0$ respectively, so that the mean velocities in both regions may become uniform and parallel to the horizontal axis everywhere. We imposed free-slip boundary conditions on the upper and lower walls parallel to the flow and periodic boundary conditions on the inlet and outlet boundaries. The free-slip boundary condition is realized by making the particles incoming to a boundary reflect specularly.
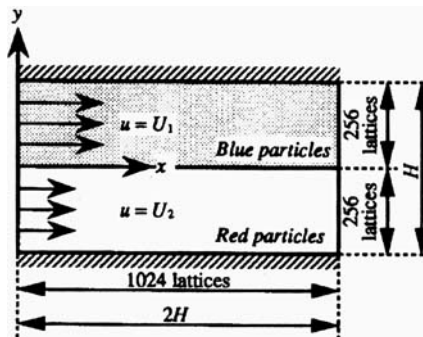

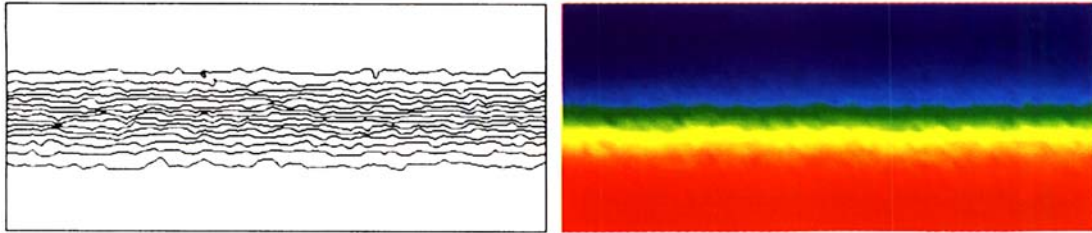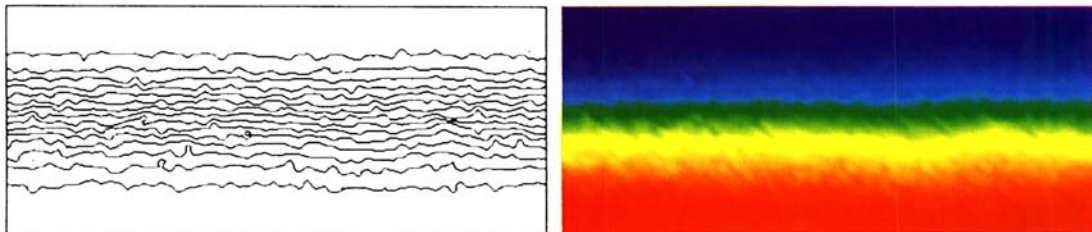Figure 3. Computational domain

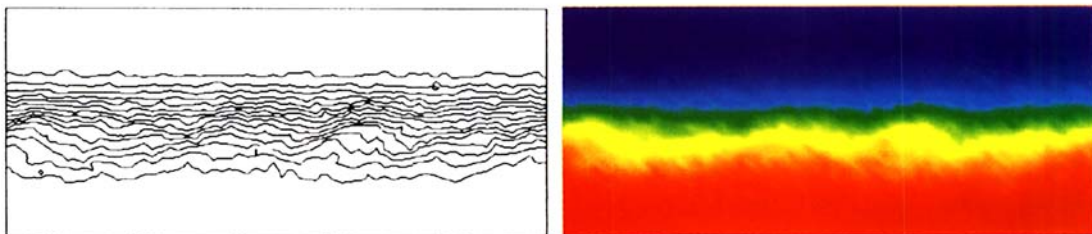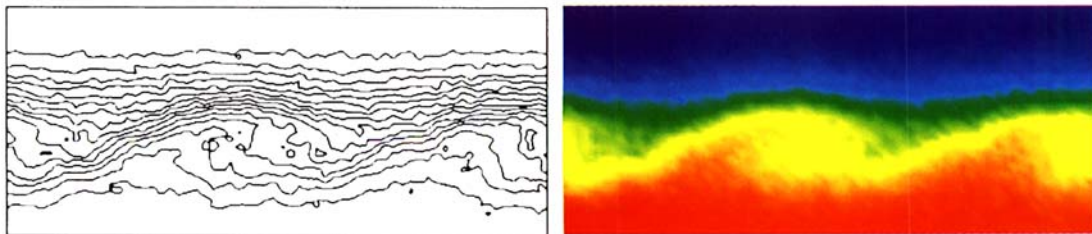(i)at 5000 time step

(ii)at 10000 time step

(a)$U_1 = 0.4, U_2 = 0.2$

(i)at 5000 time step

(ii)at 10000 time step

(b)$U_1 = 0.4, U_2 = 0.0$

Plate 1. Isoconcentration lines of red particles from $C = 0.0625$ to 0.9375 and colour maps corresponding to distribution of coloured particles. Pure red and blue colours represent $C = 1.0$ and 0.0 respectively

We performed numerical simulations for two cases, (a) $U_1 = 0.4$, $U_2 = 0.2$ and (b) $U_1 = 0.4$, $U_2 = 0.0$. We calculated the development of shear layers until the 10,000th time step in each case.

3.2. Profiles of mean velocities

We calculated the mean velocities by averaging over 16×16 sites at 2000, 4000, 6000, 8000 and 10,000 time steps. Figure 4 shows the relationship between the dimensionless co-ordinates $\eta = y/\sqrt{(vt)}$ and the horizontal components of mean velocities divided by U_1 at a position $x = 1.0H$ from the inlet boundary. Note that these velocity profiles were obtained by removing the colour labels, i.e. by regarding red and blue particles as identical. Under this procedure the two-colour lattice gas model corresponds to the original FHP model. We have also plotted a theoretical solution[14] in Figure 4. Although we observe statistical numerical fluctuations in Figure 4 because the plotted profiles are instantaneous values at each time step, most of them are distributed around the theoretical solution. We thus obtain good agreement between theory and calculations. From these results we have verified that this model is valid enough to examine shear layers.

3.3. Concentration of red particles

We also calculated the concentration C of red particles by counting the number of particles of each colour over 16×16 sites at each time step. Plate 1 shows isoconcentration lines from $C = 0.0625$ to 0.9375 and colour maps corresponding to the distribution of coloured particles at 5000 and 10,000 time steps in both cases. In case (a) it is found that the distribution of isoconcentration regions is nearly laminar and stable and that uniform diffusion of different-coloured particles occurs mutually in the direction perpendicular to the flow. On the other hand, in case (b) we can clearly observe the
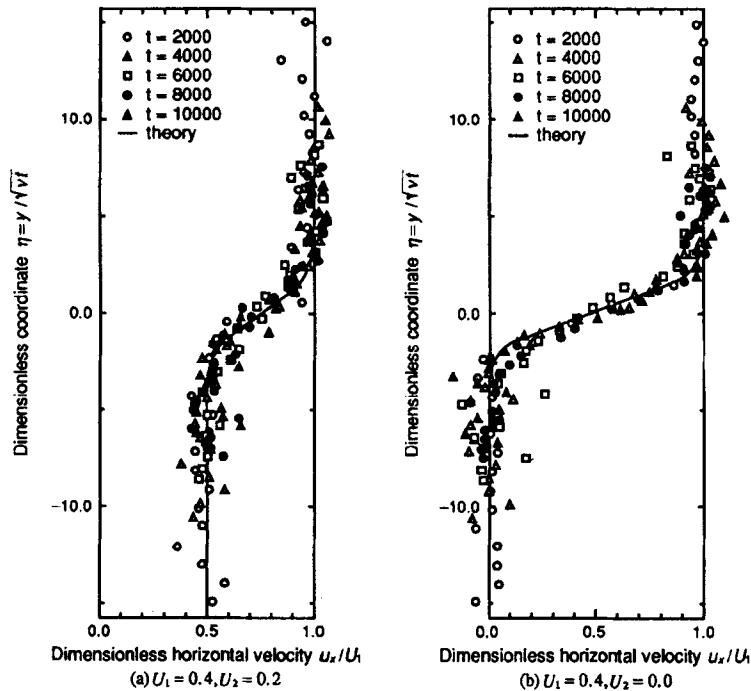

Figure 4. Horizontal velocity profiles in direction perpendicular to flow at position $x = 1.0H$ from inlet boundary at 2000, 4000, 6000, 8000 and 10,000 time steps
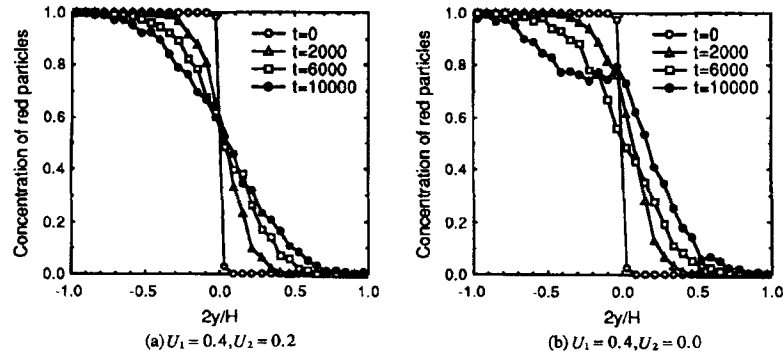
Figure 5. Concentration profiles of red particles in direction perpendicular to flow at position $x = 1 \cdot 0H$ from inlet boundary at 0, 2000, 6000 and 10,000 time steps

development of a Kelvin–Helmholtz instability at the interface between the two different-coloured fluids, as obtained in Reference 13. In this case the mixture of particles is promoted by the flow instability in addition to molecular diffusion. Figure 5 shows concentration profiles of red particles at a position $x = 1 \cdot 0H$ from the inlet boundary at representative time steps. As time goes by, the initial stepwise discontinuity of the concentration at the interface is gradually smoothed out and the concentration varies continuously within the shear layers in both cases. However, in case (b) the distribution of the concentration deviates considerably from that of ordinary diffusion phenomena. This is because the Kelvin–Helmholtz instability near the interface disturbs the uniform diffusion of particles. All discrepancies between the two cases in Plate 1 and Figure 5 are caused by the difference in relative speed between the two parallel flows.

4. CONCLUSIONS

In the present study we applied the two-colour lattice gas model to the analysis of shear layers and successfully obtained good numerical results which correspond well to the theoretical solution. Moreover, we could simulate a Kelvin–Helmholtz instability which is very similar to that observed in real phenomena. Although we need to evaluate the numerical results more quantitatively in detail, it is considered that this model is applicable to diffusion problems of mixtures of fluids.

REFERENCES

1. Y. Pomeau, *J. Phys. A: Math. Gen.*, L415–L418 (1984).
2. G. Vichniac, *Physica D*, **10**, 96 (1984).
3. N. Margolus, *Physica D*, **10**, 81–95 (1984).
4. S. Wolfram, *Rev. Mod. Phys.*, **55** 601 (1983).
5. U. Frisch, B. Hasslacher and Y. Pomeau, *Phys. Rev. Lett.*, **56**, 1505–1508 (1986).
6. S. Wolfram, *J. Stat. Phys.*, **45**, 471–526 (1986).
7. U. Frisch, D. d'Humières, B. Hasslacher, P. Lallemand, Y. Pomeau and J. P. Rivet, *Complex Syst.*, **1**, 649–707 (1987).
8. S. Wolfram, *Theory and Applications of Cellular Automata*, World Scientific, Singapore, 1986.
9. N. Margolus, T. Toffoli and G. Vichniac, *Phys. Rev. Lett.*, **56**, 1694–1696 (1986).
10. A. Clouqueur and D. d'Humières, *Complex Syst.*, **1**, 585–597 (1987).
11. D. d'Humières and P. Lallemand, *Complex Syst.*, **1**, 599–632 (1987).
12. C. Burges and S. Zaleski, *Complex Syst.*, **1**, 31–50 (1987).
13. D. d'Humières, P. Lallemand and G. Searby, *Complex Syst.*, **1**, 633–647 (1987).
14. G. K. Batchelor, *An Introduction to Fluid Dynamics*, Cambridge University Press, Cambridge, 1967.